

Calibrating bead displacements in optical tweezers using acousto-optic deflectors

Karen C. Vermeulen^{a)} and Joost van Mameren^{a)}

Laser Centre and Department of Physics and Astronomy, Vrije Universiteit Amsterdam, De Boelelaan 1081, 1081 HV Amsterdam, The Netherlands

Ger J. M. Stienen

Laboratory for Physiology, Institute for Cardiovascular Research, VU Medical Center, Van der Boechorststraat 7, 1081 BT Amsterdam, The Netherlands

Erwin J. G. Peterman, Gijs J. L. Wuite,^{b)} and Christoph F. Schmidt

Laser Centre and Department of Physics and Astronomy, Vrije Universiteit Amsterdam, De Boelelaan 1081, 1081 HV Amsterdam, The Netherlands

(Received 7 October 2005; accepted 16 December 2005; published online 30 January 2006)

Displacements of optically trapped particles are often recorded using back-focal-plane interferometry. In order to calibrate the detector signals to displacements of the trapped object, several approaches are available. One often relies either on scanning a fixed bead across the waist of the laser beam or on analyzing the power spectrum of movements of the trapped bead. Here, we introduce an alternative method to perform this calibration. The method consists of very rapidly scanning the laser beam across the solvent-immersed, trapped bead using acousto-optic deflectors while recording the detector signals. It does not require any knowledge of solvent viscosity and bead diameter, and works in all types of samples, viscous or viscoelastic. Moreover, it is performed with the same bead as that used in the actual experiment. This represents marked advantages over established methods. © 2006 American Institute of Physics. [DOI: 10.1063/1.2165568]

I. INTRODUCTION

The optical trap¹ has become an important and versatile tool in biophysics.^{2,3} In many experiments trapped beads serve as handles for proteins, cytoskeletal filaments, or DNA. In other applications trapped particles are immersed in polymer networks to perform (micro)rheology, or are used to manipulate cells.^{4–12} The displacement of a bead in a trap is a measure of the forces working on it, and can report on the viscous and elastic properties of what is attached to the bead or what surrounds it.^{13,14} Bead movement is often detected using back-focal-plane (BFP) interferometry.^{15,16} In this method, the intensity distribution of the trapping laser in the BFP of the condenser (typically) used to collect the laser light downstream from the trap is imaged on a quadrant photodiode (QPD). The normalized difference signals from the quadrants depend linearly on the lateral displacement of the bead in the plane normal to the optical axis close to the trap center.

In order to relate the voltage output of the detector electronics to displacements and forces, the detector has to be calibrated accurately and the trap stiffness has to be determined. A widely used method to measure the detector calibration factor consists of moving a fixed bead over a known distance across the laser beam waist, while recording the signals from the QPD.^{16–19} Apart from the advantage of a direct measurement, this method also has several disadvantages:

(i) calibration is usually not performed with the same bead and not at the same position in the sample as the actual experiment, the latter being especially important when the focus gets distorted with increasing distance from the surface due to spherical aberration;^{20,21} (ii) it is critical, but difficult in practice, to position the fixed calibration bead correctly with respect to the laser in x , y , and z directions; and (iii) the proximity of the cover slip could influence the measured response.

One can also determine the calibration factor from the power spectral density (PSD) of the Brownian motion of a bead confined by the trap in a viscous fluid.^{22,23} If bead diameter, fluid viscosity, and temperature are known, the PSD of Brownian motion is exactly predictable and can be used to calibrate the measured displacements of the bead in the trap. Although this method is less direct than the one described above, it has the advantage that the same bead can be used for calibration and experiment if one works in a purely viscous medium, and that one can calibrate at the very position in the sample where the experiment takes place. However, this method depends on the precise knowledge of the bead diameter, temperature, and the local viscous-drag coefficient. The latter is often not accurately known when trapping is near a surface, or when heating of the solvent by the laser changes temperature and viscosity.²⁴

We have developed a method to determine detector calibration factors directly and in all types of samples. Using acousto-optic deflectors (AODs), we scan the trapping laser rapidly across the bead, such that the bead cannot follow the trap (see Fig. 1). After a few oscillation periods, the laser is

^{a)}These authors contributed equally to this work.

^{b)}Electronic mail: gwuite@nat.vu.nl

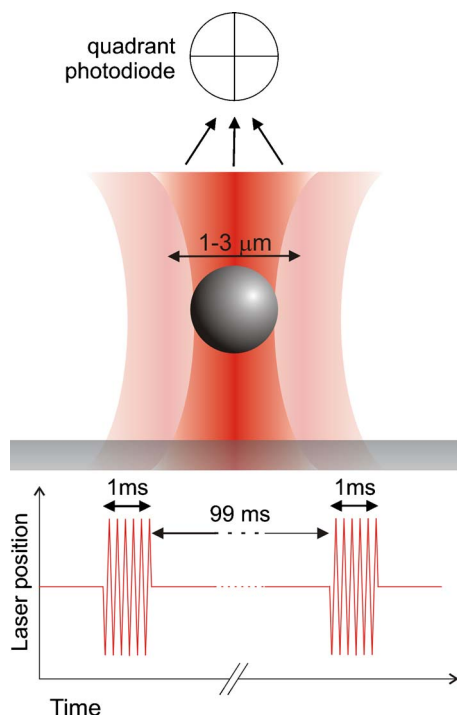


FIG. 1. (Color online) Schematic sketch of the detector calibration method. The trapping laser is periodically scanned across the bead for short periods of time (~ 1 ms) over known distances ($\sim 1\text{--}3\ \mu\text{m}$), while a quadrant photodiode (QPD) detects the response to the position change relative to the bead.

held stationary for a fixed time to allow the bead to relax into the potential minimum again before the next burst of oscillations. A pair of orthogonal AODs allows us to calibrate the detector response in two directions, normal to the optical axis. This method is related to the first method described above, but by moving the laser instead of the bead, the calibration can be directly integrated into most experiments. This avoids problems of bead polydispersity, location of the trap in the sample, or the bead in the trap. Furthermore, knowledge of exact bead diameter or local viscosity is not required. The latter can be useful in, for example, trapping experiments in viscoelastic media.¹⁴

Our calibration approach is different from the one introduced recently by Lang *et al.*,²⁵ in which AODs were used to move the bead with the trapping laser while measuring the detector response with a second, weaker detection laser. That method will not work when the bead cannot be freely moved in the sample, in, for instance, dense viscoelastic media, or with beads attached to cells. An AOD-based laser scanning scheme has also been used to create a line trap.²⁶ In the specific case of a line trap, the position of a trapped bead along the scanning direction can be measured directly.

Here, we compare our method to that using the power spectrum. We verified that the results of our method do not depend on the details of the laser scanning. We also show that the calibration factor strongly depends on the distance of the bead to the surface when a refractive index mismatch at the surface distorts the shape and size of the focus due to spherical aberration. This effect is directly related to the decrease of trap stiffness due to spherical aberration, when using an oil-immersion objective.^{17–20,27,28}

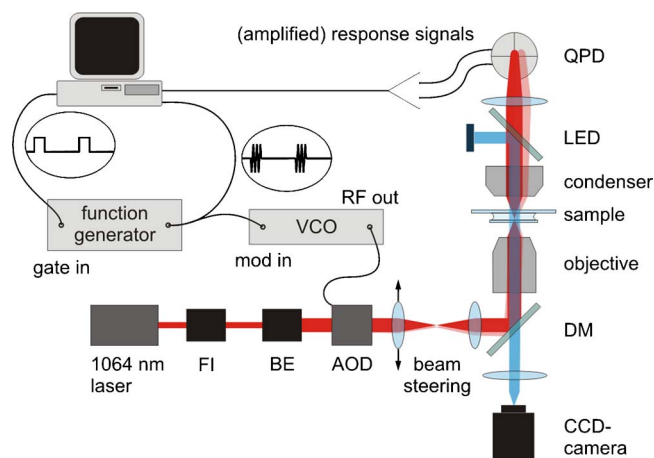


FIG. 2. (Color online) Experimental setup. The 1064 nm laser beam, directed through a Faraday isolator (FI) and a beam expander (BE), can be deflected in two directions by a set of acousto-optic deflectors (AODs). The radio-frequency input signal for the AOD crystal is generated by a voltage-controlled oscillator (VCO). The modulation signal for the VCO is a triangular wave generated by a function generator, gated in turn by a TTL signal from a computer. The laser beam is coupled via a dichroic mirror (DM) into either a $60\times$ water-immersion or a $100\times$ oil-immersion objective which focuses the laser into the sample. The transmitted light through the sample is then collected by a condenser, the back focal plane of which is imaged onto a quadrant photodiode (QPD) with one additional lens. Signals from the QPD and the modulation signal from the function generator are recorded by the computer. A blue LED illuminates the sample, the image of which is collected by a CCD camera.

II. METHODS

A. Experimental setup

The experiments were performed in a custom-built inverted microscope as depicted in Fig. 2. A Nd:YVO₄ laser (1064 nm 10 W cw, Millennium IR, Spectra Physics, Mountain View, CA), directed through a Faraday isolator (IO-3- λ -VHP, Optics For Research, Caldwell, NJ) and expanded by a beam expander ($2\text{--}8\times$, Linos Photonics GmbH & Co.KG, Göttingen, Germany), was used for trapping. A 1:1 telescope system was implemented for coarse beam steering in the sample.²² Two orthogonal AODs (DTD 276HD6, IntraAction, Bellwood, IL) were placed just before this telescope. The first-order deflected beam in both directions was then coupled via a dichroic mirror (1020dclp, Chroma Tech Corp., Rockingham, VT) into a $60\times$ water-immersion objective [Plan Apo $60\times$, numerical aperture (NA)=1.20, Nikon], or alternatively, for depth dependence experiments, into a $100\times$ oil-immersion objective (Plan Fluor $100\times$ /NA=1.30, Nikon). Here, we characterize this calibration method in one of the two scanning directions available with our AODs, yet the method can be readily extended to two-dimensional calibration of the detector response. For displacement detection, the intensity profile in the back focal plane of the condenser (Achr-Apl N, NA = 1.4, Nikon) was imaged onto a QPD (YAG444-4A, Perkin Elmer, Vaudreuil, Canada).¹⁵ We used this special purpose *p*-type, silicon QPD, operated at a reverse bias voltage of 100 V, to avoid suppression of high-frequency signals.²⁹

For fine control of the sample surface with respect to the trap, a piezo stage (P-517.3CL Physik Instrumente,

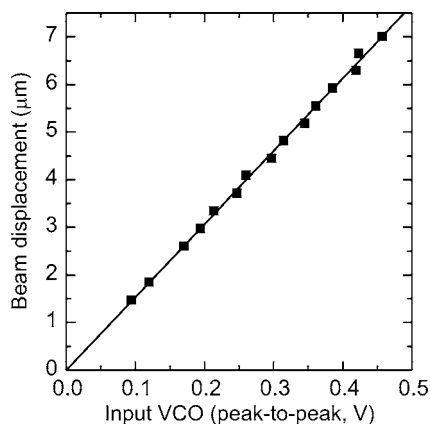


FIG. 3. Dependence of the displacement of the trap in the sample on the input modulation voltage to the VCO (5 kHz square wave from a function generator). The distance between the beads in the two time-shared traps is plotted as a function of VCO square-wave amplitude. A straight line fit is shown [fit parameters: $y = (15.3 \pm 0.2)x + 0.0 \pm 0.1$].

Karlsruhe/Palmbach, Germany) and a digital piezo controller (E-710.4CL, Physik Instrumente) were used.

To rapidly steer the laser trap using the AODs, we used a voltage-controlled oscillator (VCO) (model AA.DRF.40, AA Opto-Electronics, St. Remy les Chevreuse, France) as the source for the radio frequency signal that drives the AODs (see Fig. 2). The gated, triangular-wave output of a function generator

(LFG-1310, Leader, Cypress, CA) was used as input for the VCO, as detailed in the next section. The gate signal for the function generator was computer controlled using a computer interface board (NI PCI-6221, National Instruments, Austin, TX).

The displacement of the trap in the sample chamber as a function of the input voltage on the VCO was characterized using a continuous 5 kHz square wave as input for the VCO to generate two (time-shared) optical traps. Two beads were held in these traps and their microscope image was digitized using a frame grabber board (IMAQ PCI-1409, National Instruments). With a LabVIEW program employing template-directed pattern matching we measured the distance between the two trapped beads as a function of the peak-to-peak voltage of the input signal. Figure 3 shows the trap displacement as a function of the input voltage on the VCO when using the 60 \times water-immersion objective. The relation is linear, as expected, and its slope is independent of the distance to the surface. The same measurement was performed with the 100 \times oil-immersion objective. Also in this case the slope did not depend on the distance to the surface. Note that the ratio of the slopes found with the oil- and water-immersion objectives is consistent with the magnification factors of the two objectives.

B. Experimental procedures

Beads (silica, 0.906 μm diameter, Kisker, Steinfurt, Germany) were diluted in de-ionized water to a final concentration of $2.5 \times 10^{-5} \% (w/v)$ and infused into a sample chamber made from a cover slip and a microscope slide glued together with two narrow strips of double-stick tape. Except when noted otherwise, all measurements were performed at

10 μm distance from the surface, a position at which the viscous-drag coefficient for beads of this size is hardly influenced by the surface. The x, y , and total intensity signals of the QPD, as well as the input signal of the VCO, which can be related to the position of the optical trap, were recorded for 3 s at a sampling rate of 195 kHz using a data acquisition board (AD16 module on a ChicoPlus PCI board, Innovative Integration, Simi Valley, CA).

The triangular-wave input signal of the VCO was gated on for about 1 ms within a total cycle of 100 ms. During this 1 ms period the laser was swept at an oscillation frequency of 5 kHz across the bead 12 times (six full periods), after which the trap remained stationary for 99 ms. In most experiments, the corner frequency of the trap (which is a measure for the trap stiffness) was 300 Hz. With each data set, we also performed the same routine without a trapped bead, i.e., we recorded QPD signals immediately after releasing the bead from the trap in order to detect the small, but reproducible bead-independent signal on the QPD produced by the AOD sweep itself, which was then used to correct the data with bead. We have found the slope of this signal to be independent of most experimental parameters; hence, it needs to be characterized only once to enable off-line correction. To exclude effects of polydispersity in the bead diameter, we used the same bead for a complete data series in successive measurements, recapturing the bead after recording the background signal.

As explained in the Introduction, the detector calibration factor can also be determined from the amplitude of the power spectral density of the Brownian motion of the bead in the trap.^{22,23} To compare our measurements to the power-spectrum-based detector calibration, the Brownian motion of the same bead was also recorded without moving the trapping laser for 3 s at a sampling rate of 195 kHz.

C. Data analysis

Using a custom-written LabVIEW program, typically 60–120 sweeps of the laser across the bead were extracted from the data. The response signal was then scatter plotted against the VCO driving signal to yield (a part of) the typical S-shaped detector response curve [Fig. 4(a)].¹⁵ Except when single sweeps were analyzed, an average response curve was calculated by binning and averaging the raw data into 15–20 equidistant points along the displacement axis, followed by spline interpolating to 200 points [Fig. 4(a)]. The bead-independent signal was extracted from the data without bead in the same way, and could be fitted with a straight line [Fig. 4(a)]. The slope of the background signal did not change significantly from day to day and sample to sample, with an average background slope of $11.4 \pm 1.6 \text{ mV}/\mu\text{m}$ (s.d., $N = 40$). The magnitude of the slope is significantly smaller than the real response signal ($\sim 1000\times$). The detector response curves are corrected for the background signal using this line fit [Fig. 4(b)]. The maximal (absolute) slope should occur in the response curve when the center of the trap passes the center of the bead. The detector calibration factor in m/V (for small displacements) is thus taken to be the reciprocal of this maximal slope which in magnitude corre-

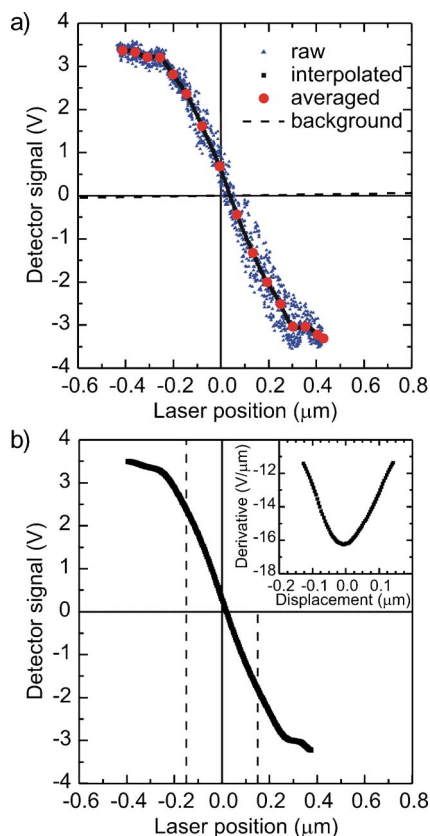


FIG. 4. (Color online) (a) Example of scatter plotted raw data of the detector response for a $0.9 \mu\text{m}$ silica bead at $10 \mu\text{m}$ from the surface. The amplitude of the laser scan across the bead was $\sim 0.4 \mu\text{m}$; the frequency of scanning was 5 kHz . The corner frequency of the trap was 300 Hz . This particular example contains the data of 19 bursts of 0.4 ms (~ 60 scans). Besides the raw data the averaged and interpolated data are also shown. The dashed line represents the reproducible background signal obtained by scanning the laser without a bead. (b) The interpolated data obtained in (a) were corrected for the slope of the background signal [dashed straight line in (a)] to give the detector signal. The derivative of this signal is shown in the inset. The maximal negative slope gives (the inverse of) the calibration factor, which in this case was found to be $6.16 \times 10^{-8} \text{ m/V}$. The vertical dashed lines indicate the linear region where the detector response deviates by less than 5% from a straight line fit to the data.

sponds to the minimum of the derivative shown in the inset in Fig. 4(b).

To independently extract the distance calibration factor from the power spectral density data, we used a LabVIEW program that calculates analytically an uncalibrated diffusion coefficient D from the Brownian displacement signal of the bead in the trap.²³ We then find the calibration factor by comparing the uncalibrated D with the expected D for a bead in physical units $D = k_B T / \gamma$,^{30,31} with γ the Stokes viscous-drag coefficient.

III. RESULTS

To validate our method, we first compared it with the power spectrum calibration method. In Fig. 5 we show the distribution of values found from repeated measurements with both methods on the same bead. We see excellent quantitative agreement between both methods (both methods: $136 \pm 4 \text{ nm/V}$). Hence, the reproducibility of our method [as for the power spectrum (PS) method] is $\sim 3\%$.

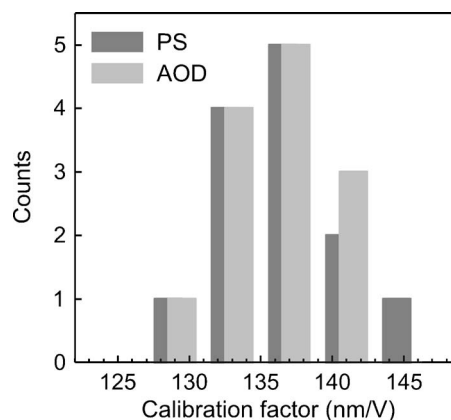


FIG. 5. Distribution of calibration values found from repeated measurements on the same individual bead with both the power spectrum (PS) and AOD calibration methods. Both methods give a detector calibration factor of $136 \pm 4 \text{ nm/V}$.

We tested the sensitivity of the calibration factor found with the AOD method to experimental parameters chosen in the procedure. In all tests a $0.9 \mu\text{m}$ silica bead was trapped $10 \mu\text{m}$ above the surface. Two effects caused by bead motion during the scans could bias the results: (i) the beads are dragged along with the moving trap to some extent and (ii) the bead diffuses during the scans. The distance over which the bead follows the passing laser trap is expected to be proportional to laser power and to the time over which the force acts in each sweep. This, in turn, is determined by frequency and amplitude of the sweeps. We checked for this effect by varying laser power such that the corner frequency ranged between 300 Hz and the full sweep frequency of (in this case) 1 kHz . We confirmed that the calibration factor was independent of laser power in this range (data not shown). Furthermore, we observed that the calibration factor was independent of the sweep frequency with which we scanned the laser across the bead in the range from 500 Hz to 10 kHz (see Fig. 6). We used sweep amplitudes of $1.5 \mu\text{m}$ and a corner frequency of 300 Hz . In a frequency regime well below the corner frequency the bead will follow the trap. Frequencies higher than 10 kHz yield insufficient data

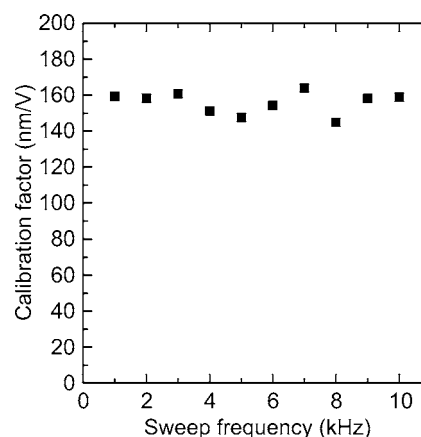


FIG. 6. Dependence of the calibration factor on the sweep carrier frequency measured with $0.9 \mu\text{m}$ silica beads at $10 \mu\text{m}$ to the surface. The corner frequency of the trap was 300 Hz . Each data point represents an average value derived from 20 bursts of 1 ms (see Sec. II).

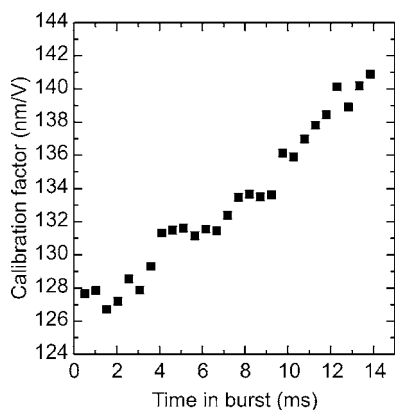


FIG. 7. Dependence of the calibration factor on time elapsed since the start of the burst. The calibration factor was determined for consecutive blocks of four sweeps across a $0.9\ \mu\text{m}$ silica bead at a distance of $10\ \mu\text{m}$ to the surface. Each data point shown here is an average over the respective four-sweep segments from ten consecutive bursts of 14 ms. The sweep frequency was 5 kHz and the trap corner frequency was 300 Hz.

points in the linear-response region due to the finite sampling frequency of 195 kHz. We observed that for amplitudes of the laser sweep larger than the bead diameter, the data become less reproducible, presumably because of periods of free diffusion when the trap has moved beyond the bead.

The duration of the burst of oscillations determines how far the bead can diffuse out of the original trap center during the burst. Diffusion in a lateral direction parallel to the sweep direction is unimpeded by the laser, but does not affect the measured response as long as the distance diffused remains small compared to the linear range of the response. The latter should indeed be the case since diffusion gives a displacement of typically 50 nm in 1 ms, while the linear range of the trap [taken here as the region where the response deviates less than 5% from a straight line, see vertical dashed lines in Fig. 4(b)] extends to ~ 150 nm. Diffusion in the other two directions is counteracted by the oscillating trap, but less strongly than by the stationary trap. Therefore it leads to a systematic decrease of the response (resulting in an increase of the detector calibration factor). To test if our experiments suffer from this effect, we varied the duration of the burst and the amplitude of the sweep, with fixed laser power and sweep frequency, and we evaluated consecutive sweeps within the bursts separately. A slight dependence on the time elapsed since the start of the burst could be observed within bursts longer than 1 ms (see Fig. 7). This result sets an upper limit of approximately 1–2 ms for the burst duration. It is thus better to average over a large number of short bursts than a small number of long bursts. For all other data in this study the burst length was 1 ms or shorter.

Figure 8 shows the focusing depth dependence of the calibration factor for the water and oil-immersion objectives. The calibration factor found for the $60\times$ water-immersion objective was approximately constant over a large range of distances to the surface. The influence of spherical aberration on the calibration factor when using the $100\times$ oil-immersion objective is evident in Fig. 8, showing that the detector sensitivity decreased by 30% over a range of $30\ \mu\text{m}$.

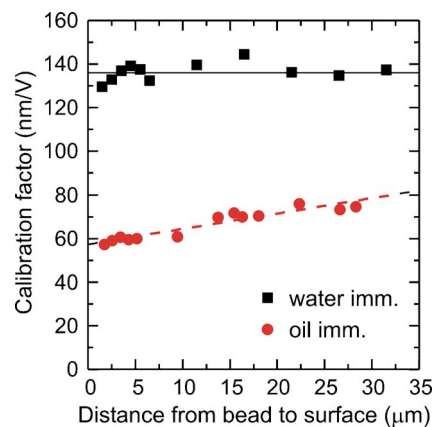


FIG. 8. (Color online) Depth dependence of the calibration factor using the $60\times$ water-immersion (squares) and the $100\times$ oil-immersion objective (circles), for $0.9\ \mu\text{m}$ silica beads. The corner frequency of the trap was 300 Hz, and the scanning frequency was 5 kHz. Every data point represents an average value derived from 20 bursts of 1 ms.

IV. DISCUSSION

Optical trapping combined with force and displacement detection has been developed from a qualitative and initially inaccurate tool to a rather precise one over recent years.²³ Accuracy of better than 5% or even 1% is of course not always needed, and a variety of convenient methods give calibration accuracies of 20%–40%. These methods are often indirect, meaning that a few beads are tested as representative for a whole batch, that the solvent in which the calibration is done may not be the same as the one in the actual experiment, or that the method requires known input parameters such as solvent viscosity, temperature, or bead diameter. If such accuracy is not good enough to, for example, precisely measure the force exerted by a molecular motor or to measure thermal fluctuations in techniques such as microrheology,^{13,14} the most prominent sources of error have to be avoided. The method described here does this in a convenient way. The calibration factor for each individual bead used in experiments can be determined. Moreover, both the position of the bead within the laser focus and its location in the sample chamber are the same as during the experiments. As an example of the importance of this we showed the expected and observed depth dependence of the calibration factor due to spherical aberrations when using an oil-immersion objective. Our method is robust because it does not depend on the details of the laser scanning. At the same time it is rapid (typically a few seconds measuring time) and independent of further experimental parameters such as viscosity, temperature, or bead diameter, which can cause uncertainties in other in-solution calibration methods.

ACKNOWLEDGMENTS

The authors wish to thank Jan Fritz (Pathology, VU Medical Center) and Heidi de Wit (Center for Neurogenomics and Cognitive Research, VU and VU Medical Center) for technical help. This work is part of the research programme of the Stichting voor Fundamenteel Onderzoek der Materie (FOM), which is financially supported by the Nederlandse Organisatie voor Wetenschappelijk Onderzoek (NWO).

- ¹A. Ashkin, J. M. Dziedzic, J. E. Bjorkholm, and S. Chu, *Opt. Lett.* **11**, 288 (1986).
- ²K. C. Neuman and S. M. Block, *Rev. Sci. Instrum.* **75**, 2787 (2004).
- ³C. Bustamante, J. C. Macosko, and G. J. L. Wuite, *Nat. Rev. Mol. Cell Biol.* **1**, 130 (2000).
- ⁴M. D. Wang, M. J. Schnitzer, H. Yin, R. Landick, J. Gelles, and S. M. Block, *Science* **282**, 902 (1998).
- ⁵G. J. L. Wuite, S. B. Smith, M. Young, D. Keller, and C. Bustamante, *Nature (London)* **404**, 103 (2000).
- ⁶K. Svoboda, C. F. Schmidt, B. J. Schnapp, and S. M. Block, *Nature (London)* **365**, 721 (1993).
- ⁷J. T. Finer, R. M. Simmons, and J. A. Spudich, *Nature (London)* **368**, 113 (1994).
- ⁸D. E. Smith, S. J. Tans, S. B. Smith, S. Grimes, D. L. Anderson, and C. Bustamante, *Nature (London)* **413**, 748 (2001).
- ⁹B. Schnurr, F. Gittes, F. C. MacKintosh, and C. F. Schmidt, *Macromolecules* **30**, 7781 (1997).
- ¹⁰K. M. Addas, C. F. Schmidt, and J. X. Tang, *Phys. Rev. E* **70**, 021503 (2004).
- ¹¹I. M. Tolic-Norrelykke, E. L. Munteanu, G. Thon, L. Oddershede, and K. Berg-Sorensen, *Phys. Rev. Lett.* **93**, 078102 (2004).
- ¹²B. van den Broek, M. C. Noom, and G. J. L. Wuite, *Nucleic Acids Res.* **33**, 2676 (2005).
- ¹³F. Gittes and C. F. Schmidt, *Curr. Opin. Solid State Mater. Sci.* **1**, 412 (1996).
- ¹⁴F. C. MacKintosh and C. F. Schmidt, *Curr. Opin. Colloid Interface Sci.* **4**, 300 (1999).
- ¹⁵F. Gittes and C. F. Schmidt, *Opt. Lett.* **23**, 7 (1998).
- ¹⁶M. W. Allersma, F. Gittes, M. J. deCastro, R. J. Stewart, and C. F. Schmidt, *Biophys. J.* **74**, 1074 (1998).
- ¹⁷A. Buosciolo, G. Pesce, and A. Sasso, *Opt. Commun.* **230**, 357 (2004).
- ¹⁸E. L. Florin, A. Pralle, E. H. K. Stelzer, and J. K. H. Horber, *Appl. Phys. A: Mater. Sci. Process.* **66**, S75 (1998).
- ¹⁹L. P. Ghislain, N. A. Switz, and W. W. Webb, *Rev. Sci. Instrum.* **65**, 2762 (1994).
- ²⁰K. C. Vermeulen, G. J. L. Wuite, G. J. M. Stienen, and C. F. Schmidt, *Appl. Opt.* (in press).
- ²¹G. J. L. Wuite, R. J. Davenport, A. Rappaport, and C. Bustamante, *Biophys. J.* **79**, 1155 (2000).
- ²²K. Svoboda and S. M. Block, *Annu. Rev. Biophys. Biomol. Struct.* **23**, 247 (1994).
- ²³K. Berg-Sorensen and H. Flyvbjerg, *Rev. Sci. Instrum.* **75**, 594 (2004).
- ²⁴E. J. G. Peterman, F. Gittes, and C. F. Schmidt, *Biophys. J.* **84**, 1308 (2003).
- ²⁵M. J. Lang, C. L. Asbury, J. W. Shaevitz, and S. M. Block, *Biophys. J.* **83**, 491 (2002).
- ²⁶R. Nambiar, A. Gajraj, and J. C. Meiners, *Biophys. J.* **87**, 1972 (2004).
- ²⁷W. H. Wright, G. J. Sonek, and M. W. Berns, *Appl. Opt.* **33**, 1735 (1994).
- ²⁸H. Felgner, O. Muller, and M. Schliwa, *Appl. Opt.* **34**, 977 (1995).
- ²⁹E. J. G. Peterman, M. A. van Dijk, L. C. Kapitein, and C. F. Schmidt, *Rev. Sci. Instrum.* **74**, 3246 (2003).
- ³⁰F. Gittes and C. F. Schmidt, *Eur. Biophys. J.* **27**, 75 (1998).
- ³¹F. Gittes and C. F. Schmidt, in *Methods in Cell Biology* (Academic, New York, 1998), Vol. 55, p. 129.